# A bioluminescence reporter mouse model for visualizing and quantifying CD8+ T cells *in vivo*

Kimberly Bettano [a,1,*]; Mark Zielstorff [b,1];
Raquel Sevilla [a]; Ruojing Yang [b]; Heather Zhou [c];
Thomas Rosahl [b]; Jie Zhang-Hoover [b]; Lily Y. Moy [b];
Weisheng Zhang [a,*]

[a] Translational Imaging
[b] Quantitative Biosciences
[c] Genome and Biomarker Sciences, Merck & Co., Inc., Kenilworth, NJ, USA

## Abstract

Cytotoxic CD8+ T cells are the primary effector cells mediating anti-tumor responses. *In vivo* monitoring of CD8+ T cells has broad implications for the development of novel cancer therapies. Here we describe the development of a genetically engineered mouse model (GEMM) in which CD8+ T cells are labeled with an optical reporter, enabling *in vivo,* longitudinal monitoring using bioluminescence imaging (BLI). Firefly luciferase (Luc2), human diphtheria toxin receptor (DTR), and enhanced green fluorescence protein (eGFP) cDNAs are engineered under the CD8$\alpha$ promoter to generate a transgenic mouse line. Luciferase mRNA and CD8$\alpha$ mRNA were generally correlated in various tissues from these mice. Sorted splenic CD8+ T cells, CD4+ T cells and CD3- non-T cells verified that the luciferase signal is specific to CD8+ T cells. *In vivo* imaging showed that luciferase signal was detected in various immune organs, such as lymph nodes, thymus, and spleen, and the detection was confirmed by *ex vivo* examination. Administration of diphtheria toxin markedly reduced luciferase signal systemically, confirming the function of the DTR. In the MC38 mouse syngeneic model, we observed significant increases in CD8+ T cells with mDX400 treatment, an anti PD-1 mouse monoclonal antibody that correlated with tumor growth inhibition. This novel reporter GEMM is a valuable drug discovery tool for profiling compounds and understanding mechanisms of action in immunotherapy of cancer.

## Introduction

CD8+ T cells are an essential component of the adaptive immune system. Specifically, cytotoxic T cells are a subpopulation of MHC class I-restricted T cells which are responsible for killing virally infected and cancerous cells.[1] It has been established that CD8^{+} T cells are required for effective antitumor immunity and their differentiation and infiltration into the tumor microenvironment (TME) play a crucial role in the prognosis of cancer.[2-4] CD8+ T cells may be inhibited through the expression of co-inhibitory receptors expressed on tumor cells, such as programmed death ligand-1 (PD-L1) and CD80. These receptors interact with programmed death (PD-1)

and cytotoxic T lymphocyte antigen-4 (CTLA-4) effectively blocking their activation and function.[1,5] Because of this phenomenon, understanding the mechanism and timing of infiltration and differentiation of CD8+ T cells into the TME aids us in the development of efficacious treatments.[6]

Clinically, it is important to understand the immune response in the TME solicited by treatments such as immunotherapy upon both diagnosis and throughout the treatment process to plan, and potentially alter, the most effective therapy throughout the course of treatment.[1] To assess the TME, immunohistochemistry (IHC) for molecular and immune markers can be used on tumor biopsy as well as flow and Cytometry by time of flight (CyTOF) to phenotype the cells that comprise the tumor.[7,8] These same techniques are used in preclinical *in vivo* models. While effective, there are limitations to these methods. Analysis of the tumor requires that the mouse be euthanized, and the tumor harvested, and processed for analysis through cell staining for flow, CyTOF, or sectioning and slide preparation for IHC. More mice need to be added to the study to have statistically significant group numbers and the data lacks the longitudinal timeline to observe temporal infiltration of specific cells into the TME. To alleviate these limitations, our goal was to develop a genetically engineered reporter mouse model in which CD8+T cells can be visualized and quantified in their native microenvironment. Tracking these cells will allow us to assess

the temporal profile CD8+ T cells and quantify their populations, i*n vivo,* using bioluminescence imaging (BLI).[5] This tool helps us understand the mechanism of action of immunomodulatory treatments in enhancing the tumor cytotoxic immune response and establish translatable immune response PD biomarkers in Immuno-Oncology studies.

*In vivo* imaging technologies play an important role in cancer clinical trials. Radiotracer-based molecular imaging technologies such as positron emission tomography (PET) and single photon emission tomography (SPECT) are more widely used to elucidate specific immune cell populations, tissue distribution, metabolic state, target expression, and cytokine production, compared to other imaging modalities, such as computed tomography (CT), ultrasound, and magnetic resonance imaging (MRI).[9] For example, [89Zr]Zr-oxine labeled therapeutic natural killer cells and cytotoxic T cells were non-invasively tracked by PET/CT in patients.[10] Recently, it has been reported that a radiolabeled minibody 89Zr-IAB22M2C against CD8+ T cells targeted specifically CD8+ T cell populations in cancer patients.[11] [99mTc]Tc-HYNIC-IL-2 accumulation in primary tumors was utilized to image CD25+ activated T-lymphocytes after pembrolizumab and ipilimumab treatments in metastatic melanoma patients.[12] FDG PET measures the metabolic states of cells and is also proposed for assessing tumor response to immunotherapy.[13] There have been many successful developments that explore imaging the immune system in pre-clinical mouse models. Radiotracers for imaging of CD3+, CD4+, CD8+ T cell populations in mice were developed to predict tumor growth response to Anti-CTLA-4 treatment.[14] Development of PET tracers for OX40 and IL2 receptors were suggested as biomarkers of T cell activation and both demonstrated a high uptake in lymphoid tissue.[15] Granzyme B and Interferon-$\gamma$ tracers were also reported for studying immune cell functions in mice and can serve as a quantitatively useful predictive biomarker for efficacious treatments.[16] However, given challenges in throughput and complexity of the PET and SPECT technologies, bioluminescence imaging (BLI) becomes a promising methodology in pre-clinical animal models for understanding the biology of the immune system, tumor microenvironment and mechanism of action in drug discovery. A transgenic reporter line in which a human IL-6 promoter drives the luciferase reporter allows for the assessment the chronic inflammatory status in various diseases using BLI.[17] The TLR2-Fluc-AcGFP transgenic was generated to study regulation of IL-10 through TLR2 signaling.[17] Mx2-Luc transgenic mouse model was used for studying temporal and spatial resolution of Type I and III interferon responses.[18] A knock-in IFN-$\beta$-luc mouse model allows scientists to interrogate how type I interferon (IFN) was produced *in vivo* and revealed influenza viral induced tissue-specific induction of IFN-beta.[19] More recently, the IFN-$\gamma$-BAC-luciferase reporter transgenic was introduced for tracking induction in autoimmune and other infectious disease settings.[20] For immune cell tracking, the FoxP3-luciferase-based transgenic was created for visualizing Foxp3+CD4+ regulatory T cells (Tregs) *in vivo*.[21] Kleinovink et al. 2019 developed a dual color imaging mouse model that allows imaging of T cell populations and their function simultaneously.[22] Until recently, attempts to visualize CD8+ T cell populations has been limited to tracking *ex vivo* labeled CD8+ T cells that were adoptively transferred.[23,24] As cytotoxic CD8+ T cells are the key component in the tumor microenvironment for anti-tumor activity, it is important to study the kinetics of CD8+ T cell trafficking and responses to immunotherapies. A knock-in CD8$\alpha$ mouse model comprising of Akaluciferase-2A-EGFP has been reported a month prior to our submission.[25] While NIR AkaLumine may emit a brighter signal, it also has an abundance of hepatic background signal which interferes with other luminescence signal in the surrounding regions.[26] The location and intensity of this signal make visualizing and quantifying signal from subcutaneous flank tumors difficult and inaccurate, necessitating the implantation of tumors towards the shoulder and neck region. In this manuscript, we describe a genetically engineered mouse line in which firefly luciferase (Luc2), diphtheria toxin receptor (DTR), and enhanced green

fluorescence protein (eGFP) reporter cassette is under the control of CD8$\alpha$ promoter in a mouse bacterial artificial chromosome (BAC) clone. This line is referred to as CD8$\alpha$-LDG. We demonstrated that the luciferase reporter is specifically expressed in CD8+ T cells, the function of T cells is unchanged, and the kinetics of infiltration of CD8+ T cells in "hot" tumors and responses to therapies was visualized and quantified.

## Materials and Methods

### Animal Reassurance Statement

All *in vivo* studies were humanly conducted with the oversight of the MRL-Boston IACUC in accordance with the *Institute for Laboratory Animal Research's Guide for the Care and Use of Laboratory Animals.*

### Reporter Cassette Synthesis and Mouse Breeding

*Luc2-P2A-DTR-P2A-eGFP reporter cassette (LDG) development:* The Luc2-P2A-DTR-P2A-eGFP reporter cassette was synthesized by fusing the firefly luciferase Luc2 (Promega), human diptheria toxin receptor (DTR), and enhanced green fluorescent protein (eGFP) cDNAs spaced by P2A self-cleavage peptide DNA sequences. The synthesized reporter cassette was cloned under the synthetic CAG promoter into pcDNA3.1+ expression vector (Thermo Fisher Scientific).

*In vitro expression of the Luc2-P2A-DTR-P2A-eGFP reporter cassette:* SH-SY5Y cells were plated into a 6-well plate and kept at 37°C overnight. At 90% confluency, cells were transfected with 2μg of either the empty vector pcDNA3.1+ or pcDNA3.1-CAG-LDG per well for 3 repeated wells using lipofectamine 2000 transfection reagent kit (Thermo Fisher Scientific) following the protocol. Twenty-four hours post transfection, D-luciferin in phosphate buffered saline (PBS) was added into each well at 150mg/L. The plate was imaged using IVIS Spectrum (Perkin Elmer). After bioluminescence imaging, fluorescence images were recorded using the EVOS Cell Imaging System (Thermo Fisher Scientific).

*Generation, genotyping, and gene profiling of CD8$\alpha$-LDG founders:* The CD8$\alpha$-LDG transgenic founder mice were generated at Taconic Biosciences. The Luc2-P2A-DTR-P2A-eGFP reporter cassette (LDG) was engineered into the BAC clone #RP23-439E18 by fusing the translation start codon ATG of the mouse CD8$\alpha$ gene with the start codon of the firefly luciferase cDNA (Luc2). The final construct containing 174Kb of 5'- upstream flanking region of the CD8$\alpha$ gene, 11kb of LDG cassette and 40Kb of 3'- downstream flanking region of the CD8$\alpha$ gene. The fragment was microinjected into the pronucleus of fertilized eggs that were collected from C57BL/6 mice. The founders were identified by PCR from tail tip DNA using primers against the Luc2 reporter gene. Gene expression profiling of founder lines was performed at Taconic Biosciences using RT-PCR by comparing mRNA transcriptional patterns of the endogenous CD8$\alpha$ and the reporter Luc2 gene from liver, spleen, muscle, blood, and bone marrow.

### Transcriptional assessment of the LDG reporter cassette in splenocytes

*mRNA transcription of Luc2, DTR and eGFP:* Genomic DNAs and RNAs from collected animal samples were purified by AllPrep DNA/RNA Kits (Qiagen) as described by the manufacturer's protocol. cDNA synthesis was performed using SuperScript™ III First-Strand Synthesis kit (Thermo Fisher Scientific) following the manufacturer's protocol to reverse transcribe mRNA into cDNAs. Real time RT-PCR was performed to measure cDNAs and genomic DNAs from the samples using TaqMan™ Universal PCR Master Mix (Thermo Fisher Scientific) and Taqman probes against GFP (Thermo Fisher Scientific; Mr03989638_mr), luciferase (Thermo Fisher Scientific; Mr03987587_mr), and human diphtheria toxin receptor (customer made Taqman primer and probe) following the manufacturer's protocol. HT9700

was used to perform real time PCR to automatically generate the Ct (cycle threshold) for each gene. GAPDH in each sample was measured to normalize the test genes mRNA and genomic DNA levels. Ratio of mRNA levels to genomic DNA levels of each gene was used to compare the 2 genes expression under the control of the same promoter.

### Interrogation of Reporter Gene Function

*In Vivo Bioluminescence Imaging:* Whole body luciferase signal was assessed in the founder line using BLI. For *in vivo* imaging, five mice at a time were anesthetized with 3% Isoflurane (Covetrus) in 100% oxygen and given a dose of 100µl of a 30mg/mL solution of Xenolight D-luciferin (Perkin Elmer) dissolved in PBS subcutaneously (150mg/kg). Mice were placed on the heated (37 °C) shelf of the imaging chamber of the IVIS Spectrum (Perkin Elmer) system and maintained on 3% Isoflurane via nose cones attached to the internal anesthesia manifold. Acquisition exposure time was 1 minute. Following the scan, mice were removed and placed back into their respective cages for sternal recovery. Luciferase signal was quantified using LivingImage Software 4.5.5 (Perkin Elmer).

*Bioluminescence Ex Vivo Tissue Survey:* Mice were anesthetized and whole-body perfused with PBS. Organs were harvested, rinsed in PBS and gently blotted on a paper towel before placing in a 6-well plate containing 2mLs of 150mg/L Luciferin and bathed for 5 minutes. Organs were blotted on a paper towel again to remove excess Luciferin and placed on black construction paper for imaging. Individual organ signal was quantified by placing regions of interest around each organ using LivingImage Software.

*Harvesting and Labeling Splenocytes for Flow Cytometry and in vitro Luciferase Assay:* Wildtype and CD8α-LDG mice were humanely euthanized with $CO_2$ inhalation according to Animal Care and Use Harmonized Guidelines and spleens were collected and kept on ice. Spleen was pulverized using the blunt end of a syringe and flushed through a 40µm filter with 10mLs of cold PBS. Red blood cells in the splenocyte suspension were lysed with RBC Lysis Buffer (Invitrogen). After 5 minutes of centrifugation at 500g, remaining cells were suspended in stain buffer (BD Biosciences) and labeled with antibodies to sort them into CD4+ (BD Biosciences), CD8+(BioLegend) and non CD3+ (BioLegend) populations using flow cytometry (FACSAria III, BD Biosciences).

*In Vitro Luciferase Assay:* An *in vitro* luciferase assay was performed on splenic cells of wildtype and CD8α-LDG mice. 100,000 cells from sorted CD4+, CD8+ and non CD3+ populations each population were plated in 100µl of Dulbecco's Modified Eagle Medium (Gibco Laboratories) in a black, 96-well clear bottom plate. Five µl of 30mg/mL Luciferin was added to each well and imaged in the IVIS Spectrum for 2 minutes. Individual wells were quantified using LivingImage Software.

*Diptheria Toxin Administration Study:* To confirm the functionality of the DTR, wildtype and CD8α-LDG mice were ventrally shaved and dosed with 18µg/kg diptheria toxin (Sigma) intraperitonially (IP), for 3 consecutive days, and tracked daily with BLI. Whole body imaging signal from the ventral side was quantified using LivingImage Software

### Tumor Studies and Immune Characterization

*MC38 Tumor Response Study:* Eight week old female CD8α-LDG transgenic and wild type littermate mice were subcutaneously inoculated in the right flank with $5 \times 10^6$ MC38 colon adenocarcinoma cells (Southern Research Institute) in 100µL phenol red free DMEM (Gibco Laboratories). Tumors were measured via caliper until they reached volumes between 80 and 120 mm³ (Volume = Length x Width x Width x 0.5). Mice were then stratified into treatment groups based on tumor volume with uniform group averages of approximately 100mm³Mice were dosed intraperitoneally with 5mg/kg of either murine anti-PD1 antibody mDX400

or an isotype control antibody (Merck & Co., Inc., Kenilworth, NJ, USA internally generated antibodies) every five days. *In vivo* bioluminescence imaging was performed as described previously throughout the study.

### Immune Characterization of CD8α-LDG Mice

*Anti-CD3 T cell activation model:* Eight week old female CD8α-LDG transgenic and wild type littermate mice were dosed IP with either 5µg anti-CD3 antibody (Bio X Cell) or isotype control antibody (polyclonal Armenian hamster IgG; Bio X Cell). Mice were euthanized four hours post dose and blood was collected in $K_3$EDTA microtubes (Greiner Bio-One North America). Blood samples were centrifuged at 1000g for 10 minutes and plasma was collected for cytokine analysis via electrochemiluminescence (Meso Scale Diagnostics).

*Delayed type hypersensitivity model:* Eight week old female CD8α-LDG transgenic and wild type littermate mice were sensitized with either sterile PBS or an emulsion of 250µg keyhole limpet hemocyanin (MilliporeSigma). KLH emulsion is generated by diluting KLH stock to 7.5mg/mL in sterile PBS and then adding equal parts by volume incomplete Freund's adjuvant and complete Freund's adjuvant (Thermo Fisher Scientific), for a final concentration of 2.5mg/mL. The components are then emulsified using a tissue homogenizer (Cole-Parmer LabGEN 125) at 30,000 RPM for three to five minutes. All components are refrigerated at 4ºC prior to use and kept on ice for the duration of the preparation and until the time of injection. Seven days later ear thickness was measured via caliper, followed immediately by intradermal injection in the ear of either 10µL sterile PBS or 10µL of 1mg/mL KLH diluted in sterile PBS (all components refrigerated and kept on ice). Ear thickness was then measured 24 hours, 48 hours, and 72 hours post ear injection by caliper.

### Statistical Analysis

Data are presented in the text and figures as means ± standard error about the mean. Student's T-tests were conducted to evaluate statistically significant differences between groups. *, **, and ***, statistical significances at P < 0.05, P < 0.01, and P < 0.001 compared with the corresponding control mice or treatment groups.

## Results

### Tissue and cellular-specific expression of Luciferase reporter cassette in the CD8α-LDG mice

To study homeostasis, proliferation, and trafficking of CD8+ T cells in mice, we generated a transgenic reporter mouse line using a mouse bacterial artificial chromosomal clone (BAC) containing the mouse CD8α gene. We first generated a reporter cassette Luc2-P2A-DTR-P2A-eGFP (LDG) for tracking CD8+ T cells using luciferase-based bioluminescence imaging, depleting CD8+ T cells by diphtheria toxin treatment, and performing flow analysis using a GFP marker. The reporter cassette was engineered under a strong synthetic CAG promoter[27] and tested in SY5Y cells using transient transfection. Strong luciferase activity and weak GFP signal was detected (Suppl. Fig. 1). The reporter cassette was then engineered under the mouse CD8α promoter (Fig. 1A) and transgenic CD8α-LDG founders were identified. Transcription of endogenous CD8α and luciferase reporter Luc2 genes in various tissues was analyzed using RT-PCR. The pattern of luciferase mRNA transcription generally corelated well with the endogenous CD8α mRNA pattern with an exception that high Luc2 mRNA and low CD8α mRNA were observed in muscle (Suppl. Fig. 2).
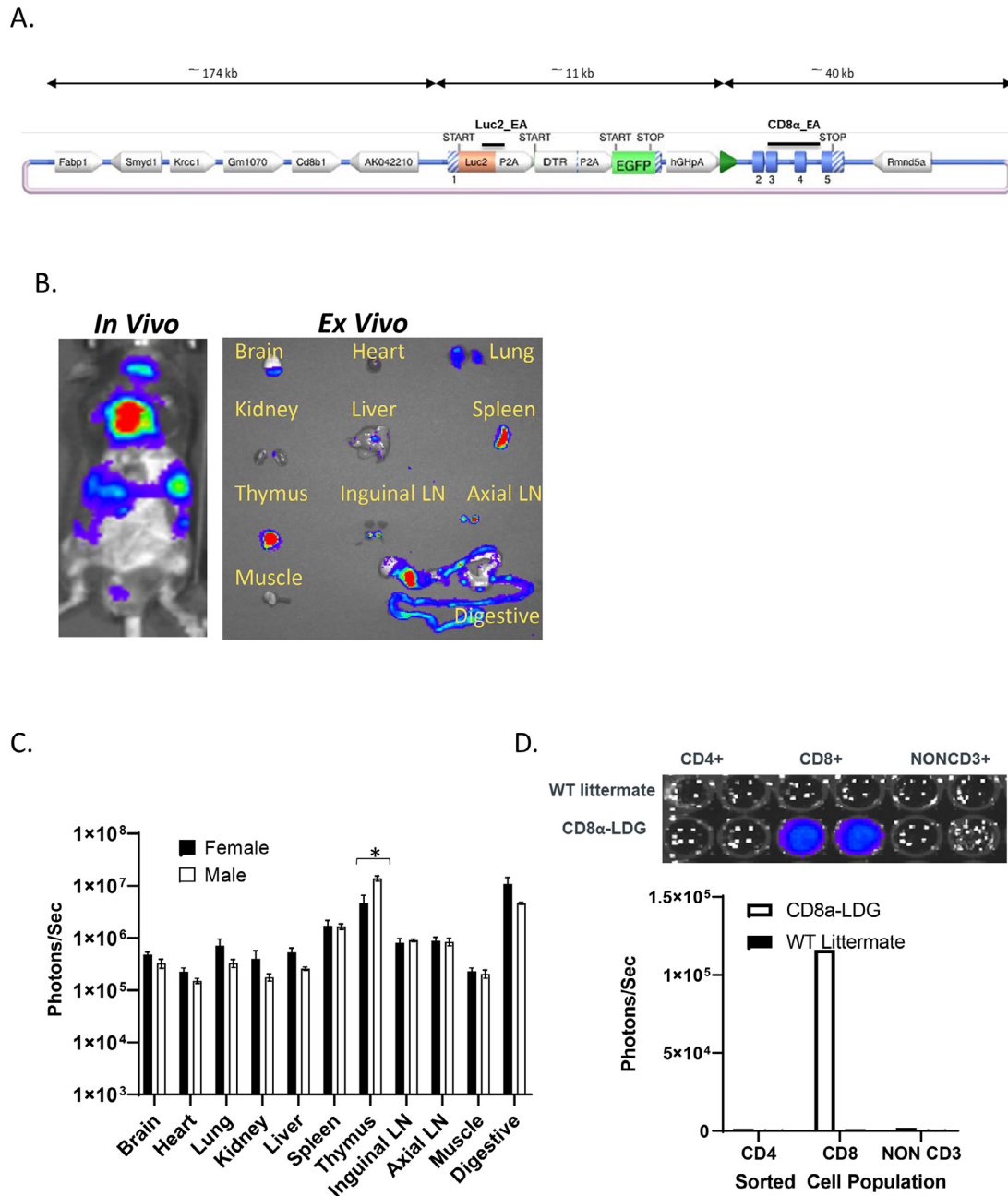
**Figure 1.** Tissue and cellular specificity of Luc2 reporter expression *A.* Mouse genomic locus shows the insertion point of the reporter cassette and BAC clone. *B.* CD8+ T cell luciferase signal observed *in vivo* is confirmed with *ex vivo* tissue imaging. *C.* Luciferase signal from various tissues were quantified in photons per second using LivingImage software and plotted as mean ± standard error (n =3). * indicates statistical significance at P < 0.05 between male and female thymus with a Student's T-test. *D.* CD4+ T cells, CD8+ T cells, and non-CD3 T cells were sorted from splenocytes of CD8α-LDG (n=3) and wildtype (n=3) littermates using flow cytometry and pooled cells were imaged with the IVIS Spectrum in duplicate in a 96 well black plate.

To examine tissue distribution of CD8+ T cells, mice were imaged from both ventral and dorsal sides. The ventral image of a CD8α-LDG mouse shows that luciferase expressing CD8+ T cells were mainly emanating from immune organs, such as lymph nodes, thymus, and spleen. (Fig. 1B). There was no significant gender difference observed with the exception of the thymus (Suppl. Fig. 3 & Fig. 1C). To confirm the origin of luciferase signal, tissues were collected, and *ex vivo* imaging confirmed high signal observed from spleen, thymus, and axial, inguinal, and mesenterial lymph nodes (Fig. 1B). As expected, thymus, spleen and digestive tissues showed strong luciferase signal while muscle showed very low luciferase signal (Fig. 1B&C).

However, some muscle tissues showed small hot spots, possibly from lymph nodes in the muscles (data not shown). Surprisingly, high CD8+ T cell signal was also observed from lung and cerebellum brain region.

To further confirm the luciferase signal originated from CD8+ T cells where the CD8α gene is transcribed, we sorted CD8+ T cells, CD4+ T cells, and non-CD3 T cells from splenocytes and a luciferase assay was performed Fig. 1D clearly shows the luciferase signal is exclusively expressed from CD8+ T cells.

Then we examined expression and function of DTR by IP injection of diphtheria toxin (DT). Three days of treatment of DT markedly
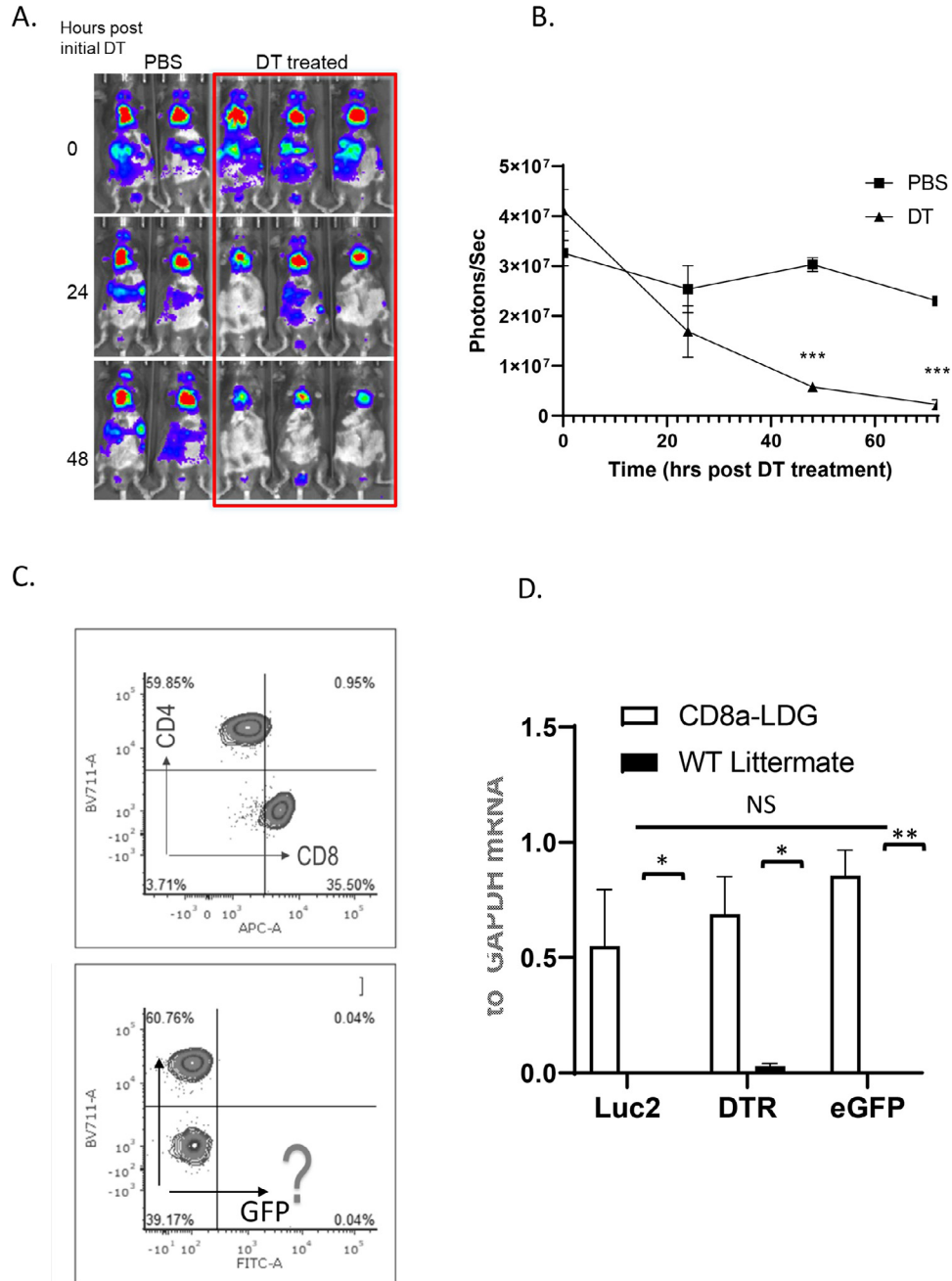
**Figure 2.** Examination of DTR and eGFP *A.* CD8$\alpha$-LDG mice were IP injected with either PBS (n=2) or 18 µg/kg of diptheria toxin (n=3) for 3 consecutive days and mice were imaged at 0 (pre-treatment), 24, 48, and 72 hours after the first treatment. Representative images are shown. *B.* Luciferase signal from the entire ventral side were quantified as described in Fig. 1 and plotted as mean + standard error. *** indicates statistical significances at P < 0.001 compared with the corresponding PBS treated mice with a Student's T-test. *C.* CD45+CD3+ cells were isolated from splenocytes of CD8$\alpha$-LDG mice and analyzed by flow cytometry. Representative biparametric cytogram plots shows populations of CD4+ and CD8+ T cells while GFP was not detectable on the FITC channel. *D.* mRNA and genomic DNA isolated from CD8$\alpha$-LDG and wildtype littermate splenocytes (n=3) confirms the presence of the Luc2, DTR and the eGFP reporter gene by comparing the ratio of mRNA levels to genomic DNA levels of each gene. There are no significant differences (NS) when comparing the mRNA of Luc2, DTR and eGFP using One-Way Analysis of Variance method. * and ** indicate statistical significances at P < 0.05 and 0.01 compared genes between CD8$\alpha$-LDG mice with the wildtype littermates, respectively, with a Student's T-test.

depleted Luciferase expression in all organs (Fig. 2A & B). DT reduced CD8+ T cell signal about 97% of baseline from $4.3\times10^7$ to $4.4\times10^5$ while signal from PBS controls was only changed from $3.2\times10^7$ to $2.1\times10^7$. However, we were not be able to detect any GFP positive cells by either fluorescence microscopy or Flow analysis. Fig. 2C shows no FITC was

detected while CD8+ T cells were observed. Splenic mRNA was analyzed for transcription levels of Luc2, DTR, and eGFP using RT-PCR, demonstrating that these three genes were equally transcribed (Fig. 2D), indicating that eGFP was not functional and might not be efficiently cleaved by the P2A peptide.
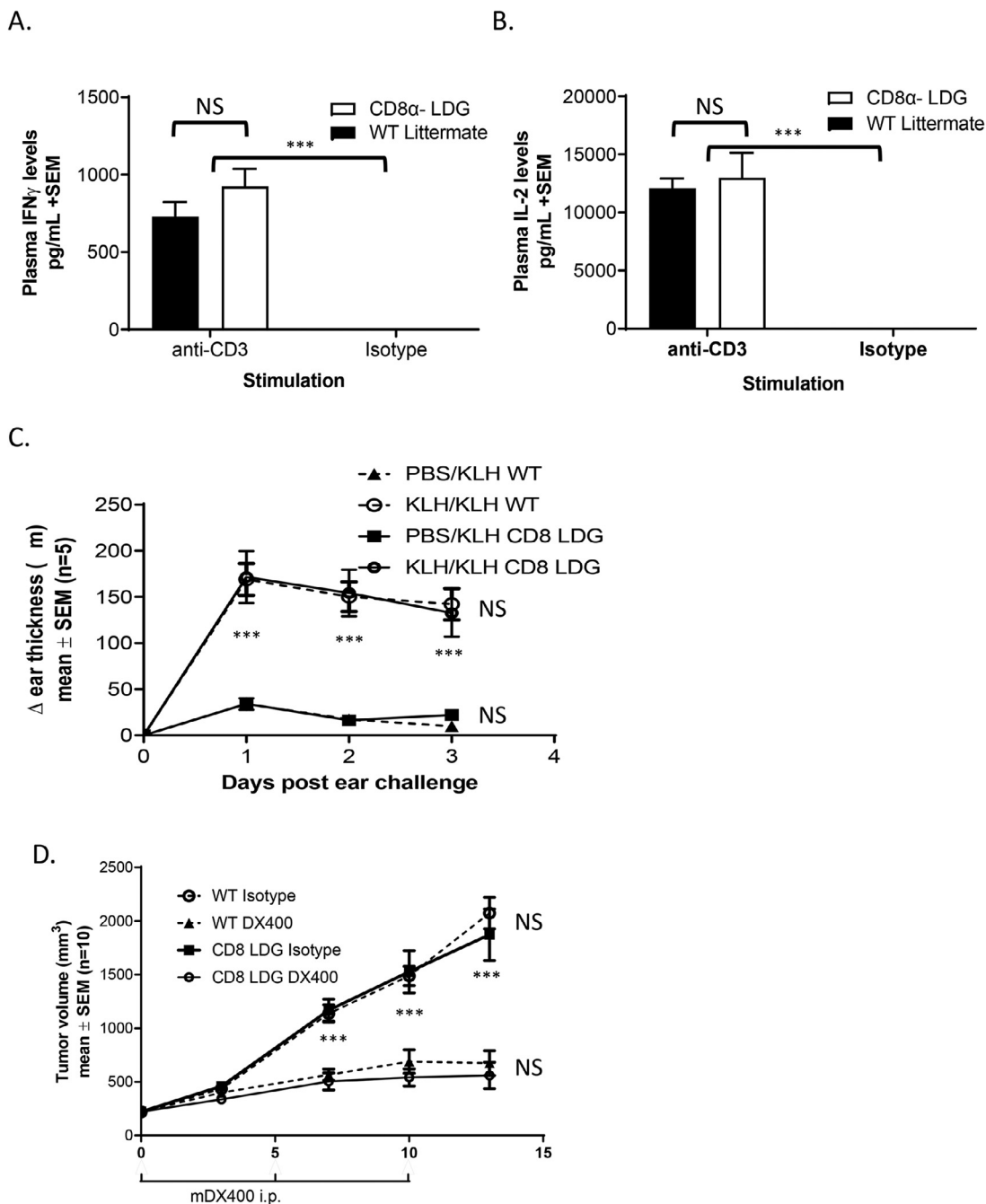
**Figure 3.** T cell function is not affected by the expression of the reporter cassette. CD8$\alpha$-LDG mice and WT mice (n=10) are IP stimulated with either 5μg of anti-CD3 monoclonal antibody or isotype control antibody and plasma samples were collected 4 hours post treatments. Plasma IFN-$\gamma$ (*A*) and IL-2 (*B*) were assayed as described in Materials and Methods and plotted as as mean + standard error. In a Delayed-Type Hypersensitivity Ear Thickness Model, ear thickness was measured by caliper following injection with keyhole limpet hemocyanin (KLH). Data are dipicted as mean + standard error of changes in ear thickness from the baseline. *D*. MC38 tumor bearing WT and CD8$\alpha$-LDG mice with average volume of about 200mm$^3$ were enrolled into two groups (n=10). Both WT and CD8$\alpha$-LDG mice were then treated with isotype controld or DX400 and tumor growth is plotted as mean ± standard error of tumor volumes. There are no significant differences (NS) between the CD8$\alpha$-LDG mice and their WT littermates in any graph in Fig 3. *** indicates significant differences between control and treated mice at p <0.001 with Student's T-test.

### Expression of LDG cassette does not impair normal CD8+ T cell function

We evaluated if expression of the reporter cassette affects the functionality of the CD8+ T cells. CD8+ T cells produce and secrete cytokines such as IFN-$\gamma$ and IL-2 when activated. We stimulated both CD8$\alpha$-LDG and wildtype mice with Anti-CD3 mouse monoclonal antibody. A single IP injection of anti-CD3 mAb strongly induced secretion of both IFN-$\gamma$ and IL-2 in plasma at the same levels in CD8$\alpha$-LDG mice and wildtype littermate controls while the isotype antibody control had no effect (Fig. 3A&B).
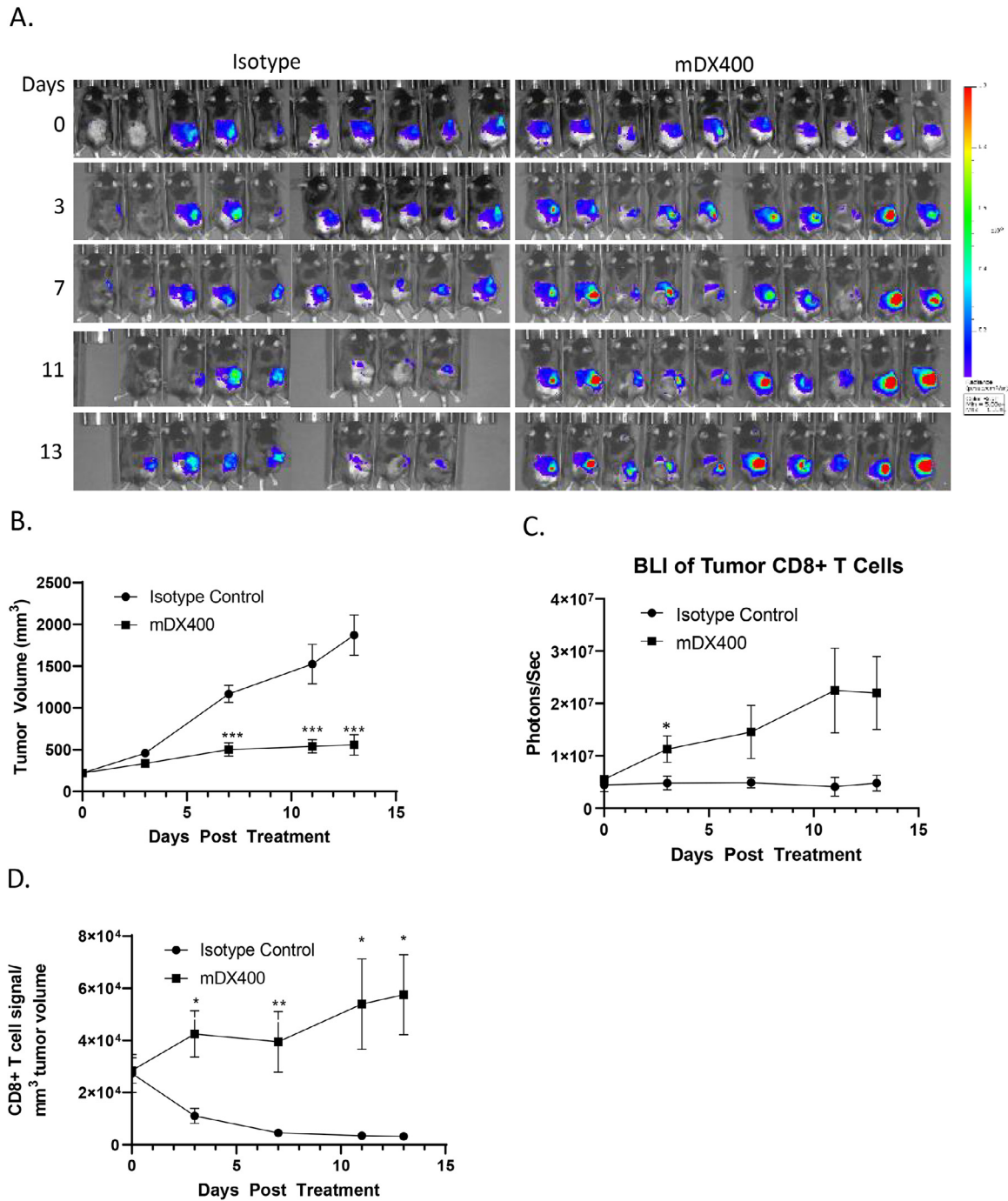
**Figure 4.** Visualization of the CD8+ T Cells in MC38 tumors *in vivo* in real time, in response to anti-PD1-mAb CD8α-LDG mice were implanted subcutaneously with MC38 tumor cells and mice with an average volume at 200mm$^3$ were enrolled into mDX400 and isotype control antibody groups (n=10). Mice were imaged using BLI at day 0 (pre-dosing), 3, 7, 11, and 13 post treatment. *A*. Bioluminescence images show the dorsal side of animals with tumor on the right flank. Luciferase signal comes from the tumor region and is displayed on the same color scale for all images. *B*. Tumor volumes (mm$^3$) were measured by caliper and plotted as mean ± standard error of tumor volumes. *C*. Tumor infiltrated CD8+ T cells were assessed by quantifying the luciferase signal in photons per second over the tumor region and plotted as mean ± standard error. *D*. CD8+ T cell density was assessed and graphed as mean ± standard error of the ratio of tumor luciferase signal to tumor volume (Photons/second/mm$^3$). For all graphs in Figure 4, *,** and *** indicate significant differences between Isotype control and mDX400 treated mice at p <0.05, P < 0.01, and 0.001, respectively with Student's T-test.

Delayed-type hypersensitivity (DTH) reactions, also known as type IV hypersensitivity reactions, are mediated by soluble or cell-associated antigens primarily involving CD4+ or CD8+ T cell activation. We further examined these CD8α-LDG mice with the KLH DTH model to test the function of CD8+ T cells. Fig. 3C demonstrated that the expression of LDG reporter genes had no effect on ear thickness in response to KLH stimulation compared to wildtype control mice.

To demonstrate that LDG reporter expression did not affect tumor growth in syngeneic mouse models, we implanted MC38 tumor cells on the flank of CD8α-LDG mice and their wildtype littermates. As shown in Fig. 3D, the growth rate of MC38 tumors in CD8α-LDG mice and the response to anti-PD-1 antibody treatment were identical to that in wildtype littermate controls.

*Visualizing CD8+ T cells in "hot" tumors and responses to therapeutics*

To visualize the kinetics of CD8+ T cells in tumor models, we choose the "hot" MC38 model to test if we can detect infiltrated CD8+ T cells in the tumor, and how the CD8+ T cells respond to a treatment with an immune checkpoint antibody, anti-PD-1 mouse monoclonal antibody, mDX400. MC38 tumor cells were implanted into the right flank of CD8α-LDG mice and mice were randomized into isotype control mouse mAb and mDX400 mAb groups (n=10) with average tumor sizes of $221+22mm^3$ and $221+19mm,^3$ respectively. Antibodies were administered once every 5 days intraperitoneally at 5mg/kg with a total of 3 doses. Tumors were calipered twice a week and bioluminescence imaging was performed once a week. As shown in Fig. 4A., basal level of luciferase signal was observed in the regions of tumor growth prior to treatment. mDX400 stimulated infiltration of CD8+ T cells as early as 3 days into treatment. mDX400 mediated about 4.0-fold increases in luciferase signal over the tumor region and the tumor volumes only increased to 2.5-fold over the 13 days of treatment (Fig. A-C). In contrast, the isotype control antibody treatment had no effect on luciferase signal (1.1-fold) while tumors significantly grew to 8.5-fold and three mice had to be euthanized due to tumor volumes on day 11 (Fig. A-C). Noticeably, some isotype control treated tumors showed decreased CD8+ T cell signal during tumor growth. When tumor infiltrated CD8+ T cell luciferase signal was normalized with its tumor volume, the density of CD8+ T cells per mm³ tumor volume was calculated, showing an 18-fold difference in infiltrated CD8+ T cells between anti-PD-1 mAb and isotype control (Fig. 4D). Interestingly, the antiPD-1 mAb mDX400 specifically mediated tumor specific CD8+ T cell infiltration while CD8+ T cells in other immune organs appeared to be unchanged (Suppl. Fig. 4).

## Discussion

We successfully developed a genetically engineered mouse model for visualizing CD8+ T cells *in vivo* in real time. As we learn more about the "tumor ecosystem," our strategy for treating cancers and developing therapies has shifted from attacking the tumor cell itself to targeting the host immune response using immunotherapies.[28] Therefore, the field of Immuno-Oncology can greatly benefit from a mouse model that can help us longitudinally interrogate the key component of tumor immune microenvironment before, during, and after treatment. The CD8α-LDG mouse model gives us the ability to assess the mechanism of action of immunomodulatory treatments in enhancing tumor cytotoxic immune response *in vivo* in real time using BLI. MC38 is a model of mouse colon cancer and is known to have a high presence of CD8+ T cells.[33] The excellent response to anti-PD1 mAb treatment with marked increased the density of CD8+ T cells in MC38 tumors in our CD8α-LDG model (Fig. 4) are not consistent with the recent data from the C57BL/6-CD8aem(IRES-AkaLuci-2A-EGFP) knock-in mice in the same tumor and with the same treatment in which anti-PD1 mAb demonstrated much less tumor growth

inhibition with no difference in CD8+ T cell density.[26] Higher luciferase signal from the liver form the C57BL/6-CD8aem(IRES-AkaLuci-2A-EGFP) mice make it challenging to study subcutaneous flank tumors. This may be a combination effect of expression of the AkaLuc reporter gene and its substrate AkaLumine.[27]

Turning an immune "cold" tumor to "hot" is a focus in Immuno-Oncology drug discovery to enhance therapeutic response and broaden the patient population that can benefit from immunotherapies. This model can elucidate whether and how a signaling pathway can upregulate the presence of CD8+ T cells in the tumor immune microenvironment (TIME) that might enhance anti-tumor activity. Studies have shown that B16F10 syngeneic tumors do not respond well to either anti-PD-1 or anti-PDL1 antibody treatments.[29,30] In contrast to MC38 tumors, we observed very little CD8+ T cell signal in B6F10 tumors, with even lower signal than surrounding tissues (Suppl. Fig. 5), consistent with findings above. We were also able to turn these immune "cold" B16F10 tumors hotter with increased tumor infiltrated CD8+ T cell signal using an agonist of the innate immune system (Data not shown).

The three genes that are driven by the CD8α promoter are all present in the transgenic mouse line. Function of Luc2 was confirmed *in vivo* with BLI and DTR was confirmed through administration of diptheria toxin in the CD8 α-LDG mice. We were unable to detect any GFP+ cells on the FITC channel from insolated CD8+ T cells (Fig. 2C). But we did observe weak eGFP fluorescence signal in transfected cells with a much stronger CAG synthetic promoter (Suppl. Fig. 1). These data suggest that it is highly likely that there was an incomplete process of the P2A self-cleavage of DTR-P2A-eGFP fusion in which the C-terminal fusion of DTR protein quenched the fluorescent function of the fluorescence protein. It is well documented that order of multiple genes and selection of 2A peptides will significantly reduce the efficiency of cleavages in polycistronic expression system.[31] While the lack of functional GFP expression in the CD8α-expressing cells hinders our ability to sort these cells, a number of effective mouse anti-CD8 antibodies are commercially available for *ex vivo* Flow analysis.

When designing a genetically engineered mouse model, it is imperative that the random insertion of the transgene does not alter the characteristics of the background mouse strain. The results of the immune characterization studies, including the assessment of IFN-γ and IL-2 following anti-CD3 treatment, and the DTH ear study suggests that the normal function of cytokines has not been affected in the CD8α-LDG model when compared to wild-type littermate mice and historical, in-house, data. MC38 is a model of mouse colon cancer and is known to have a high presence of CD8+ T cells.[32] We confirmed that there is no difference in tumor growth kinetics between the CD8α-LDG and wildtype mice by caliper measurement as well as no difference in response to mDX400 and the isotype control. Similar efficacy is observed between the CD8α-LDG and wildtype mice as confirmed with both caliper measurement and BLI which correlates to previous, in-house studies and literature. We also observed CD8+ T cells homing to tumor sites specifically after mDX400 treatment. These data assure us that the optical reporter signal measured in this model faithfully represent distribution, kinetics, and response of the endogenous CD8+ T cells.

Interestingly, when we imaged mice from the ventral side where CD8+ T cells are present in most peripheral immune tissues, we did not observe significant changes in CD8+ T cell signal (Suppl. Fig. 4). However, clinical data demonstrates that anti-PD-1 antibodies induce a plethora of immune-related adverse events (irAE) in skin, gastrointestinal tract, liver, endocrine and renal system, etc. as these irAEs can start with asymptomatic or with minimal symptoms.[33]

A large presence of CD8+ cells throughout the cerebellum relative to other brain regions was unexpectedly observed in the *ex vivo* tissue survey (Fig. 1B). Tissue-resident memory (TRM) CD8+ T cells have been reported in humans and mice and it is believed that these CD8+ TRM cells in the parenchyma of the mouse CNS provide local cytotoxic defense

against viral infections.[34,35] This phenomenon is also frequently observed in post-traumatic brain injury.[36] However, CD8+ T cells and their function in cerebellum have not been reported. Similarly, high IL-6 expression in cerebellum was observed in a luciferase transgenic mouse model in which the luciferase reporter was under the human IL-6 promoter.[17] Although it is possible that higher CD8+ T cells and IL-6 expression in the cerebellum may be an artifact of insertion of the reporter gene, it warrants more investigation to determine if this region may maintain a reservoir of CD8+ T cells and IL-6 producing immune cells, serving as a CNS lymphoid tissue and playing a role in immunosurveillance in the brain.

Although bronchus-associated lymphoid tissue (BALT), a constitutive mucosal lymphoid tissue adjacent to major airways in some mammalian species is not found in humans or mice, a similar tissue, inducible BALT (iBALT), an ectopic lymphoid tissue, can be found throughout the lung in both humans and mice when there is inflammation.[37] The CD8+ T cells observed throughout the mouse lung suggests that iBALT in mice may play more of a surveillance role. This observed signal might be due to detection sensitivity as iBALT is only observed during infection when contributing to respiratory virus resolution.[38]

In summary, we have successfully developed a tool to track and quantify CD8+ T cell populations longitudinally, *in vivo,* using bioluminescence imaging. This reporter model provides a unique tool to assess CD8+ T cell infiltration in various tumor models and can help lead to a better understanding of mechanism of action of targets and pathways for development of improved cancer immunotherapies.

## Acknowledgments

## Declaration of Conflict of Interest

## References

1. Maimela NR, Liu S, Zhang Y. Fates of CD8+ T cells in Tumor Microenvironment. *Comput Struct Biotechnol J* 2019;**17**:1–13. doi:10.1016/j.csbj.2018.11.004.

2. Gajewski TF, Schreiber H, Fu YX. Innate and adaptive immune cells in the tumor microenvironment. *Nat Immunol* 2013;**14**:1014–22. doi:10.1038/ni.2703.

3. Locy H. Immunomodulation of the Tumor Microenvironment: Turn Foe Into Friend. *Front Immunol* 2018;**9**:2909. doi:10.3389/fimmu.2018.02909.

4. Piersma S. High Number of Intraepithelial CD8 + Tumor-Infiltrating Lymphocytes Is Associated with the Absence of Lymph Node Metastases in Patients with Large Early-Stage Cervical Cancer. *Cancer Research* 2007;**67**:354–61. doi:10.1158/0008-5472.CAN-06-3388.

5. Waldman AD, Fritz JM, Lenardo MJ. A guide to cancer immunotherapy: from T cell basic science to clinical practice. *Nature Reviews Immunology* 2020;**20**:651–68. doi:10.1038/s41577-020-0306-5.

6. Nolz JC. Molecular mechanisms of CD8(+) T cell trafficking and localization. *Cell Mol Life Sci* 2015;**72**:2461–73. doi:10.1007/s00018-015-1835-0.

7. Young YK, Bolt AM, Ahn R, Mann KK. Analyzing the Tumor Microenvironment by Flow Cytometry. *Methods Mol Biol* 2016;**1458**:95–110. doi:10.1007/978-1-4939-3801-8_8.

8. Bjornson ZB, Nolan GP, Fantl WJ. Single-cell mass cytometry for analysis of immune system functional states. *Curr Opin Immunol* 2013;**25**:484–94. doi:10.1016/j.coi.2013.07.004.

9. Krekorian M. Imaging of T-cells and their responses during anti-cancer immunotherapy. *Theranostics* 2019;**9**:7924.

10. Kurebayashi Y, Choyke PL, Sato N. Imaging of cell-based therapy using 89Zr-oxine ex vivo cell labeling for positron emission tomography. *Nanotheranostics* 2021;**5**:27.

11. Pandit-Taskar N. First-in-humans imaging with 89Zr-Df-IAB22M2C anti-CD8 minibody in patients with solid malignancies: preliminary pharmacokinetics, biodistribution, and lesion targeting. *Journal of Nuclear Medicine* 2020;**61**:512–19.

12. Markovic SN. Non-invasive visualization of tumor infiltrating lymphocytes in patients with metastatic melanoma undergoing immune checkpoint inhibitor therapy: a pilot study. *Oncotarget* 2018;**9**:30268.

13. Aide N. FDG PET/CT for assessing tumour response to immunotherapy. *European journal of nuclear medicine and molecular imaging* 2019;**46**:238–50.

14. Larimer BM, Wehrenberg-Klee E, Caraballo A, Mahmood U. Quantitative CD3 PET imaging predicts tumor growth response to anti-CTLA-4 therapy. *Journal of Nuclear Medicine* 2016;**57**:1607–11.

15. van der Veen EL. Development and Evaluation of Interleukin-2–Derived Radiotracers for PET Imaging of T Cells in Mice. *Journal of Nuclear Medicine* 2020;**61**:1355–60.

16. Larimer BM. Granzyme B PET imaging as a predictive biomarker of immunotherapy response. *Cancer research* 2017;**77**:2318–27.

17. Lalancette-Hebert M, Phaneuf D, Soucy G, Weng Y, Kriz J. Live imaging of Toll-like receptor 2 response in cerebral ischaemia reveals a role of olfactory bulb microglia as modulators of inflammation. *Brain* 2009;**132**:940–54.

18. Pulverer JE. Temporal and spatial resolution of type I and III interferon responses in vivo. *J Virol* 2010;**84**:8626–38. doi:10.1128/jvi.00303-10.

19. Lienenklaus S. Novel reporter mouse reveals constitutive and inflammatory expression of IFN-β in vivo. *The Journal of Immunology* 2009;**183**:3229–36.

20. Reynolds CJ. Bioluminescent Reporting of In Vivo IFN-γ Immune Responses during Infection and Autoimmunity. *The Journal of Immunology* 2019;**202**:2502–10. doi:10.4049/jimmunol.1801453.

21. Suffner J. Dendritic cells support homeostatic expansion of Foxp3+ regulatory T cells in Foxp3. LuciDTR mice. *The journal of immunology* 2010;**184**:1810–20.

22. Kleinovink JW. A dual-color bioluminescence reporter mouse for simultaneous in vivo imaging of t cell localization and function. *Frontiers in immunology* 2019;**9**:3097.

23. Kim D, Hung C-F, Wu T-C. Monitoring the trafficking of adoptively transferred antigen-specific CD8-positive T cells in vivo, using noninvasive luminescence imaging. *Human gene therapy* 2007;**18**:575–88.

24. Hailemichael Y. Persistent antigen at vaccination sites induces tumor-specific CD8+ T cell sequestration, dysfunction and deletion. *Nature medicine* 2013;**19**:465–72.

25. Guo Y. A bioluminescence reporter mouse strain for in vivo imaging of CD8+ T cell localization and function. *Biochemical and Biophysical Research Communications* 2021;**581**:12–19. doi:10.1016/j.bbrc.2021.10.022.

26. Nakayama J. High Sensitivity In Vivo Imaging of Cancer Metastasis Using a Near-Infrared Luciferin Analogue seMpai. *Int J Mol Sci* 2020;**21**. doi:10.3390/ijms21217896.

27. Farokhimanesh S, Rahbarizadeh F, Rasaee MJ, Kamali A, Mashkani B. Hybrid promoters directed tBid gene expression to breast cancer cells by transcriptional targeting. *Biotechnol Prog* 2010;**26**:505–11. doi:10.1002/btpr.353.

28. Pitt JM. Targeting the tumor microenvironment: removing obstruction to anticancer immune responses and immunotherapy. *Ann Oncol* 2016;**27**:1482–92. doi:10.1093/annonc/mdw168.

29. Durham NM. Oncolytic VSV Primes Differential Responses to Immuno-oncology Therapy. *Mol Ther* 2017;**25** 1917-1932, doi:10.1016/j.ymthe.2017.05.006.

30. Doty DT. Modeling Immune Checkpoint Inhibitor Efficacy in Syngeneic Mouse Tumors in an Ex Vivo Immuno-Oncology Dynamic Environment. *Int J Mol Sci* 2020;**21**. doi:10.3390/ijms21186478.

31. Liu Z. Systematic comparison of 2A peptides for cloning multi-genes in a polycistronic vector. *Scientific Reports* 2017;**7**:2193. doi:10.1038/s41598-017-02460-2.

32. Efremova M. Targeting immune checkpoints potentiates immunoediting and changes the dynamics of tumor evolution. *Nat Commun* 2018;**9**:32. doi:10.1038/s41467-017-02424-0.

33. Albandar HJ. Immune-Related Adverse Events (irAE) in Cancer Immune Checkpoint Inhibitors (ICI) and Survival Outcomes Correlation: To Rechallenge or Not? *Cancers (Basel)* 2021:13. doi:10.3390/cancers13050989.

34. Smolders J. Tissue-resident memory T cells populate the human brain. *Nature Communications* 2018;**9**:4593. doi:10.1038/s41467-018-07053-9.

35. Wakim LM. The Molecular Signature of Tissue Resident Memory CD8 T Cells Isolated from the Brain. *The Journal of Immunology* 2012;**189**:3462–71. doi:10.4049/jimmunol.1201305.

36. Daglas M. Activated CD8+ T Cells Cause Long-Term Neurological Impairment after Traumatic Brain Injury in Mice. *Cell Reports* 2020;**29** 1178-1191.e1176doi:https://doi.org/10.1016/j.celrep.2019.09.046 (2019).

37. Randall TD. Bronchus-associated lymphoid tissue (BALT) structure and function. *Adv Immunol* 2010;**107**:187–241. doi:10.1016/b978-0-12-381300-8.00007-1.

38. Bivas-Benita M. Airway CD8+ T cells induced by pulmonary DNA immunization mediate protective anti-viral immunity. *Mucosal Immunology* 2013;**6**:156–66. doi:10.1038/mi.2012.59.